 

# Potential of Mean Force between Solute Atoms in Salt Solution: Effects Due to Salt Species and Relevance to Conformational Transition of Biomolecules

**Masahiro Kinoshita* and Yuichi Harano**

Institute of Advanced Energy, Kyoto University, Uji, Kyoto 611-0011

Received January 27, 2005; E-mail: kinoshit@iae.kyoto-u.ac.jp

We analyze the interaction, the potential of mean force (PMF), between solute atoms in pure water and in solutions of various salts (NaCl, KCl, KBr, and KI) using the dielectrically consistent reference interaction site model theory. As for the PMF between solute atoms with like charges, the addition of increasing concentration of salt gradually leads from repulsive to attractive interactions. When the salt concentration becomes sufficiently high, the contact of like-charged atoms is stabilized and the stability is enhanced as the magnitude of the charge increases. For positive charges, the ability of salt to change the PMF is governed by anion species and becomes higher as the anionic size increases, while for negative charges it is governed by cation species and becomes higher as the cationic size decreases. Concerning the PMF between solute atoms with unlike charges, the addition of increasing concentration of salt gradually leads from attractive to repulsive interactions. The contact of unlike-charged atoms is less stabilized than in pure water. Physical insights into these results, which are generally applicable to solvation behavior of solute molecules, are then provided and the relevance to the salt-induced conformational transition of biomolecules is discussed in detail.

Solvation behavior of a solute molecule is of crucial importance in a variety of fields such as solution chemistry, biochemistry, and biophysics. The potential of mean force (PMF) between atoms or groups constituting the solute molecule is known to provide fundamental information on the solvation behavior. In the so-called superposition approximation,[1,2] which has successfully been applied to analyses of the conformational stability of a peptide molecule in pure water, the atoms of the solute molecule are treated separately (i.e., isolated atoms are considered) and the solvation free energy plus the conformational energy of the solute molecule is regarded as the sum of the PMFs for all possible pairs of these atoms. It is true that the atom–atom or group–group PMF is not capable of describing the details that are dependent on specific chemical or conformational properties of individual solute molecules. However, some qualitative aspects, which are common in a number of different solute molecules, can be studied by analyzing the PMF.

An important point is that the PMF in salt solution is drastically different from the PMF in pure water when the atoms or groups carry partial charges. Nevertheless, systematic studies on the PMF in salt solution have not been reported yet. Most of the previously reported works considered only the PMF between alkali-halide ions in pure water (a good review is given in Refs. 3 and 4). The computer simulations are almost useless for the salt-solution system because of the limited number of water molecules. By contrast, the integral equation theories are capable of treating infinitely many water molecules and potentially allow us to analyze the PMF in salt solution with a moderate computational effort. Above all, the dielectrically consistent version of the reference interaction site model (RISM) theory[5] (the DRISM theory) combined with our powerful numerical solution algorithm[6,7] is expected to be very useful. Kovalenko and Hirata,[3,4] who employed the three-dimensional (3D) DRISM theory, calculated the $Na^+$–$Na^+$, $Na^+$–$Cl^-$, and $Cl^-$–$Cl^-$ potentials not only in pure water but also in 1 M-NaCl solution. However, the alkali-halide ions were again treated and the salt concentration was limited to 1 M. The most challenging subject is to analyze the effects of the salt species on the PMF between solute atoms with partial charges, but such an analysis has never been performed.

In the present article, solute atoms with a negative partial charge (atom A) and with a positive partial charge (atom C) are considered. The PMF is calculated using the one-dimensional (1D) DRISM theory for the A–A, C–C, and A–C pairs in pure water and in solutions of various salts (NaCl, KCl, KBr, and KI). The charges are set at zero in some of the calculations. The PMF is analyzed in detail and effects due to the salt concentration, the salt species, and the magnitude of the partial charge are systematically studied. Examining the results obtained, we give physical insights which are generally applicable to solvation behavior of solute molecules. In particular, the relevance to the salt-induced conformational transition of biomolecules is discussed for two typical examples. The first example is for peptides and proteins with many positively charged groups in the side chains. It was experimentally observed for those peptides and proteins that they are extremely unfolded under conditions of acidic pH and low ionic strength but are refolded to molten-globule-like conformations by the salt addition.[8–10] The effectiveness of salt to cause the conformational transition is strongly dependent on anion species and follows the order $I^- > Br^- > Cl^-$, the reverse Hofmeister series. That is, the effectiveness becomes higher as the anionic size increases. These properties are quite general and qualita-

Published on the web August 4, 2005; DOI 10.1246/bcsj.78.1431

Table 1. Values of $\sigma$ Used by Various Researchers

| Ion | Refs. 16, 17 | Ref. 18 | Ref. 19 | Ref. 13 | This Work |
|---|---|---|---|---|---|
| $Na^+$ | 0.229, 0.222 | 0.229, 0.222 | 0.190 | 0.190 | 0.226 |
| $K^+$ | 0.317, 0.310 | 0.317, 0.310 | 0.266 | 0.284 | 0.314 |
| $Cl^-$ | 0.395, 0.388 | 0.445 | 0.362 | 0.362 | 0.392 |
| $Br^-$ | 0.434, 0.428 | 0.462 | 0.390 | 0.392 | 0.419 |
| $I^-$ | 0.490, 0.483 | — | 0.432 | 0.440 | 0.454 |

When two numbers are given, the first one is for the combination with the oxygen atom of water and the second one is for that with the hydrogen atom. In this work the average of the two numbers is adopted.

tively the same for a variety of peptides and proteins as long as they have many positively charged groups. The second example is for DNA with many negatively charged phosphates. By increasing the salt concentration, one can induce the structural transition from the right-handed (B-DNA) to the left-handed (Z-DNA) double-stranded helices.[11,12] The ability of salt to cause the structural transition is strongly dependent on cation species and follows the order $Na^+ > K^+ > Rb^+ > Cs^+$: The ability becomes higher as the cationic size decreases, which is in marked contrast to the first example. The present study is clearly different from our earlier work[13] in which the salting-out phenomenon for a peptide-like molecule with zero net charge was considered and the ability of salt to cause the solubility decrease always followed the Hofmeister series.

## Model and Theory

**Model Potentials.** The extended simple point charge (SPC/E) model,[14] where a repulsive interaction is introduced between O and H sites,[15] is employed for water. The salts considered are NaCl, KCl, KBr, and KI. The potential forms and parameters developed by Pettitt and Rossky[16] and modified in our earlier work[17] are used for bulk water and salt solution. For the solute atom-water and -ion potentials, the Coulomb plus Lennard–Jones (LJ) form is adopted and the LJ parameters ($\sigma$ and $\varepsilon$) are calculated using the usual combination rule. For the potential between the water hydrogen atom and a solute atom, however, only the repulsive part of the LJ potential is considered. In principle, solute atoms with any sizes and correspondingly realistic magnitudes of partial charges can be treated in the present analysis. The oxygen atom in the side chain of Glu (atom A) and the hydrogen atom in the side chain of Lys (atom C) are chosen as representative solute atoms. Atom A has a negative partial charge while atom C has a positive one. The partial charge of atom A is larger than that of atom C. Atom A is larger in size as well.

The partial charges and LJ parameters for the solute atoms are taken from the AMBER-type parameters.[13] Unfortunately, for ions there is neither a reliable set of LJ parameters nor a good method for determining them. The values of $\sigma$ used by various researchers are compared in Table 1. For $Na^+$ and $K^+$, Pettitt and Rossky[16] and Yu and Karplus[18] use the same values, so these values are employed. For $Cl^-$, however, they give considerably different values. Therefore, the values given by Masterton and Lee[19] and Imai et al.[13] are also considered, and the averages of the values given by the four groups[13,16,18,19] are adopted. For $Br^-$ the value used in our earlier work[17] is fairly different from that given by Yu and Karplus, so the average of the values given by the four groups[13,17–19] is employed. Similarly, for $I^-$ (this was not considered by Yu and Karplus) the average of those given by the three groups[13,17,19] is adopted. The values of $\varepsilon$ are taken from our earlier work.[17] The partial charges and LJ parameters thus determined for calculating the solute atom-water and -ion potentials are collected in Table 2. The dimensionless number densities and the dielectric constants of salt solutions are determined from the experimental data.[17]

Table 2. Partial Charges and Lennard–Jones Parameters for Atomic Sites

| Site | $Q$ (—) | $\sigma$ (nm) | $\varepsilon$ (kcal/mol) |
|---|---|---|---|
| H | 0.4238 | 0.040 | 0.046 |
| O | −0.8476 | 0.316 | 0.156 |
| $Na^+$ | 1.0000 | 0.226 | 0.293 |
| $K^+$ | 1.0000 | 0.314 | 0.440 |
| $Cl^-$ | −1.0000 | 0.392 | 0.448 |
| $Br^-$ | −1.0000 | 0.419 | 0.638 |
| $I^-$ | −1.0000 | 0.454 | 0.806 |
| A | −0.7210 | 0.285 | 0.200 |
| C | 0.2940 | 0.178 | 0.020 |

**Theory.** Kovalenko and Hirata[3,4] calculated the $Na^+$–$Na^+$, $Na^+$–$Cl^-$, and $Cl^-$–$Cl^-$ potentials in pure water and in 1 M-NaCl solution. They treated a pair of ions by employing the 3D-DRISM theory. The sum of the $\Delta\mu_S$-values ($\Delta\mu_S$ denotes the solvation free energy) of isolated ions was subtracted from $\Delta\mu_S$ of the ionic pair separated by a prescribed distance. This calculation was repeated by changing the distance. The PMF thus obtained is generally more accurate than the PMF calculated via the much simpler route using the usual 1D version of the theory and the water-isolated ion correlation functions. However, the change, "PMF in salt solution"—"PMF in pure water", which is a central issue in the present article, is not significantly dependent on the calculation method. In fact, the changes calculated via the two routes are quantitatively similar to each other, as shown in Fig. 1. The discrepancies observed at small separations in the Figure are unimportant because the core repulsions dominate at those separations. In the present study, the 1D-DRISM theory[5] is employed with the hypernetted-chain (HNC) closure equations.

The calculation of the PMF between solute atoms is based on the standard procedure. It comprises the following four steps:

(1) Treat the bulk system of pure water or salt solution and calculate the solvent (water molecules and ions) correlation functions.

(2) Treat atom A immersed in pure water or salt solution at

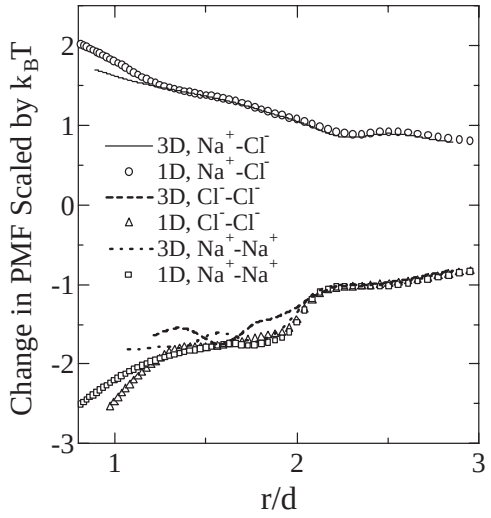


Fig. 1. Change in the PMF, "PMF in 1 M-NaCl solution"—"PMF in pure water", calculated for $Na^+$–$Na^+$, $Na^+$–$Cl^-$, and $Cl^-$–$Cl^-$ using the 1D- and 3D-DRISM theories. The change is scaled by $k_BT$. The $\sigma$-values of $Na^+$ and $Cl^-$ are 0.235 nm and 0.440 nm, respectively ($d = 0.28$ nm).

infinite dilution. Calculate atom A-solvent correlation functions.

(3) Treat atom C immersed in pure water or salt solution at infinite dilution. Calculate atom C-solvent correlation functions.

(4) Calculate A–A, A–C, and C–C correlation functions.

In step (4), because of the presence of long-range Coulombic potentials, care must be taken in the forward and back Fourier transforms of the correlation functions. The site–site Ornstein–Zernike (SSOZ) relation in the Fourier space is expressed by

$$F_{MN}(k) = 2\rho_S C_{MH}(k)H_{NH}(k) + \rho_S C_{MO}(k)H_{NO}(k) + \rho_+ C_{M+}(k)H_{N+}(k) + \rho_+ C_{M-}(k)H_{N-}(k), \quad (1a)$$

$$F_{MN}(k) = H_{MN}(k) - C_{MN}(k); \quad M, N = \mathrm{A}, \mathrm{C}, \quad (1b)$$

where $c(r)$ and $h(r)$ are, respectively, the direct and total correlation functions (the capital letters represent the Fourier transforms), $f(r) = h(r) - c(r)$, $r$ is the distance between centers of the two atomic sites considered, $k$ is the wave number, $\rho$ is the number density. The subscripts "S", "+", and "−" denote "water", "cation", and "anion", respectively. The subscripts "H" and "O" denote "H-site" and "O-site" in a water molecule, respectively. The equations:

$$\rho_O = \rho_H/2 = \rho_S, \quad (2a)$$

and

$$\rho_+ = \rho_-, \quad (2b)$$

are utilized in writing Eq. 1. From the charge neutrality condition, we obtain

$$2\rho_S q_H H_{NH}(k) - 2\rho_S q_H H_{NO}(k) = 0, \quad (3a)$$

$$\rho_+ q_+ H_{N+}(k) - \rho_+ q_+ H_{NA}(k) = -q_N. \quad (3b)$$

The equations:

$$q_O = -2q_H, \quad (4a)$$

and

$$q_- = -q_+, \quad (4b)$$

are utilized in writing Eq. 3. Here, $c_{MH}(r)$, $c_{MO}(r)$, $c_{M+}(r)$, and $c_{M-}(r)$ are decomposed into short-range and long-range terms as[6,7]

$$c_{MH}(r) = c_{MH}^{SR}(r) - q_M q_H \lambda(r)/(k_BT), \quad (5a)$$

$$c_{MO}(r) = c_{MO}^{SR}(r) + 2q_M q_H \lambda(r)/(k_BT), \quad (5b)$$

$$c_{M+}(r) = c_{M+}^{SR}(r) - q_M q_+ \lambda(r)/(k_BT), \quad (5c)$$

$$c_{M-}(r) = c_{M-}^{SR}(r) + q_M q_+ \lambda(r)/(k_BT), \quad (5d)$$

$$\lambda(r) = \mathrm{erf}(\alpha r)/r, \quad (5e)$$

where $k_BT$ is the Boltzmann constant times the absolute temperature, $\mathrm{erf}(x)$ denotes the error function, and $\alpha$ is a parameter whose order of magnitude is unity. The Fourier transform of Eq. 5 is expressed by

$$C_{MH}(k) = C_{MH}^{SR}(k) - q_M q_H \Lambda(k)/(k_BT), \quad (6a)$$

$$C_{MO}(k) = C_{MO}^{SR}(k) + 2q_M q_H \Lambda(k)/(k_BT), \quad (6b)$$

$$C_{M+}(k) = C_{M+}^{SR}(k) - q_M q_+ \Lambda(k)/(k_BT), \quad (6c)$$

$$C_{M-}(k) = C_{M-}^{SR}(k) + q_M q_+ \Lambda(k)/(k_BT), \quad (6d)$$

$$\Lambda(k) = 4\pi \exp\{-k^2/(4\alpha^2)\}/k^2. \quad (6e)$$

Substituting Eq. 6 into Eq. 1 and using Eq. 3 yields

$$F_{MN}(k) = \rho_S\{2C_{MH}^{SR}(k) + C_{MO}^{SR}(k)\}H_{NO}(k) + \rho_+\{C_{M+}^{SR}(k)H_{N+}(k) + C_{M-}^{SR}(k)H_{N-}(k)\} + q_M q_N \Lambda(k)/(k_BT). \quad (7)$$

Since $\Lambda(k) \to \infty$ as $k \to 0$, the numerical transform is performed as follows.

(a) Calculate $F_{MN}(k)$ using Eq. 7.

(b) Obtain the back transform of $\{F_{MN}(k) - q_M q_N \Lambda(k)/(k_BT)\}$.

(c) Add $q_M q_N \lambda(r)/(k_BT)$ to the result from step (b) to obtain $f_{MN}(r)$.

The PMF $\Phi_{MN}(r)$ is then obtained from

$$\Phi_{MN}(r)/(k_BT) = u_{MN}(r)/(k_BT) + s_{MN}(r), \quad (8a)$$

$$s_{MN}(r) = -f_{MN}(r), \quad (8b)$$

where $u(r)$ is the pair potential. In Eq. 8, $u(r)/(k_BT)$ and $s(r)$ are referred to as the direct interaction term and the solvation term, respectively. The solvation free energy $\Delta\mu_S$ of a solute atom is also calculated using the Singer–Chandler formula.[20] The coordination number of counterions around an isolated atom is defined by

$$n_+ = 4\pi\rho_+ \int_0^{r_{min}} r^2 g_{A+}(r)dr, \quad g_{A+}(r) = h_{A+}(r) + 1, \quad (9a)$$

$$n_- = 4\pi\rho_- \int_0^{r_{min}} r^2 g_{C-}(r)dr, \quad g_{C-}(r) = h_{C-}(r) + 1, \quad (9b)$$

where $r_{min}$ is the position of the first minimum in $g_{A+}(r)$ or $g_{C-}(r)$ calculated in step (2). In the 1 M-solution, $\rho_+ d^3 = \rho_- d^3 = 0.013224$.

A pair of solute atoms separated by distance $R$, which is treated as a supermolecule with two interaction sites, is also

immersed in pure water and in salt solution at the infinite dilution limit. The pair correlation functions for one of the solute atoms and counterions thus obtained are spherically averaged and denoted by $g^*_{A+}(r)$ and $g^*_{C-}(r)$. As $R \to \infty$, $g^*_{A+}(r) \to g_{A+}(r)$ and $g^*_{C-}(r) \to g_{C-}(r)$ for all $r$. The information on the structure of counterions near the pair of solute atoms is contained in the following:

$$\delta g_{A+}(r;R) = g^*_{A+}(r) - g_{A+}(r), \quad (10a)$$

$$\delta g_{C-}(r;R) = g^*_{C-}(r) - g_{C-}(r). \quad (10b)$$

**Numerical Method.** A sufficiently long range $r_L$ is divided into $N$ grid points ($r_i = i\delta r$, $i = 0, 1, \ldots, N-1$; $\delta r = r_L/N$) and all the functions are represented by their values on these points. $N$ and $\delta r$ are set at 4096 and $0.02d$ ($d = 0.28$ nm), respectively. The resultant nonlinear simultaneous equations are solved using our hybrid algorithm,[6,7] where the Newton–Raphson (NR) method is judiciously combined with the Picard iteration. The so-called coarse variables are converged in the inner NR loop and the fine variables are updated in the outer Picard loop. In steps (2) and (3), the Jacobian matrix is part of the input data and is kept constant. The algorithm is very powerful and for a new calculation there is no need to prepare the correlation functions that converged under another calculation condition. With the crude initial guesses given by

$$f_{MJ}(r) = \beta q_M q_J \lambda(r), \quad M = \mathrm{A}, \mathrm{C}; \quad J = \mathrm{H}, \mathrm{O}, +, - \quad (11)$$

and the severe convergence criterion,

$$E_{\mathrm{out}} = \sum_{J=\mathrm{H},\mathrm{O},+,-} \sum_{i=0}^{N-1} |f_{MJ}(i\delta r) - f_{MJ}(i\delta r)/\{4N f_{MJ}(i\delta r)\}| < 10^{-7}, \quad (12)$$

converged solutions are obtained in only 20 to 30 total NR iterations ($\alpha = 2.6$).

## Results and Discussion

**Direct Interaction Term and Solvation Term.** As Eq. 8 indicates, the PMF between a pair of solute atoms can be decomposed into the direct interaction term $u(r)/(k_BT)$ and the solvation term $s(r)$. Figure 2a shows $u_{CC}(r)/(k_BT)$ and $s_{CC}(r)$ (both in pure water and in 1 M-NaCl solution) and Figure 2b shows $u_{AC}(r)/(k_BT)$ and $s_{AC}(r)$. As the solute atoms approach each other, $s_{CC}(r)$ decreases while $u_{CC}(r)/(k_BT)$ increases, and $s_{AC}(r)$ increases while $u_{AC}(r)/(k_BT)$ decreases except at very small separations where the direct core repulsion dominates. In this sense, the direct interaction term and the solvation term are opposing. An important point is that the solvation term is enhanced by the salt addition. The absolute value of the PMF that is obtained as the sum of the two terms is two orders of magnitude smaller than the absolute values of the two terms, and thus the small change in the solvation term caused by the salt addition is crucially important. Hereafter, the two terms are simply referred to as the direct interaction and the solvation, respectively.

**Potentials of Mean Force in 1 M-NaCl Solution.** The very small separations where the core repulsion dominates are excluded from the discussion. $\Phi_{AA}(r)/(k_BT)$ is plotted in Figs. 3a and 3b. Two cases, where the full partial charge is assigned to atom A and where the charge is set at zero, respectively, are considered in pure water and in 1 M-NaCl solution. In the case of full charges in pure water, $\Phi_{AA}(r)/(k_BT)$ is repulsive except at small separations and it converges rather slowly to $u_{AA}(r)/(\varepsilon_W k_BT)$ ($\varepsilon_W$ is the dielectric constant of water). By the salt addition, $\Phi_{AA}(r)/(k_BT)$ exhibits a pronounced downward shift due to the enhanced solvation described above. It becomes short range and rapidly converges to zero. The first and second minimums correspond to the contact atom pair and the solvent-separated atom pair, respectively.[3,4] The DRISM theory overestimates the depth of the first minimum of $\Phi_{AA}(r)/(k_BT)$ both in pure water and in salt solution (the accurate PMF in pure water could be repulsive at all separations),[3,4] but the difference between the two curves is quantitatively reliable as mentioned above. When the charge of atom A is set at zero, the PMF exhibits a pattern of the so-called hydrophobic interaction. By the salt addition, the hydrophobic interaction becomes slightly stronger (the hydrophobicity of the solute atoms increases to a small extent), but the two curves in pure water and in salt solution are similar to each other. The PMF for the zero charges in pure water is considerably different from that for the full charges in salt solution.

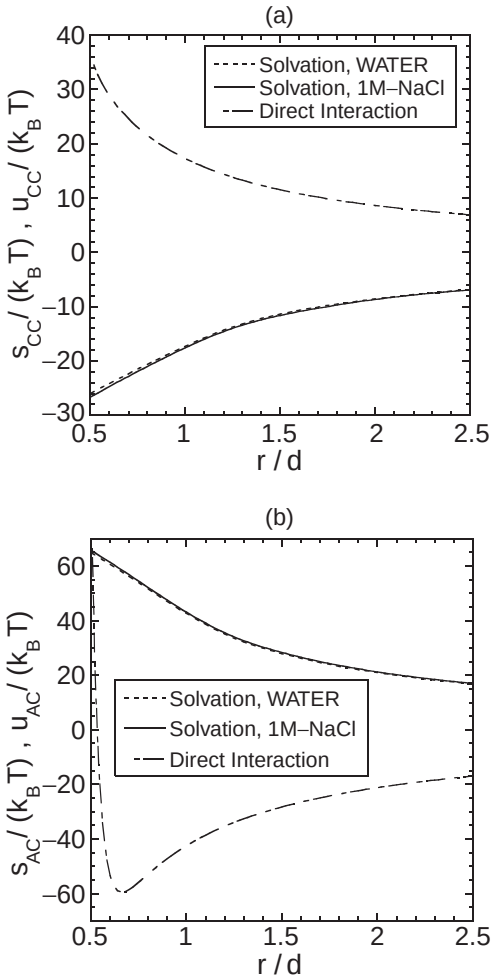


Fig. 2. Direct interaction term and solvation term defined by Eq. 8 ($d = 0.28$ nm). The full values of the partial charges are assigned to the solute atoms. (a) For the C–C pair. (b) For the A–C pair.

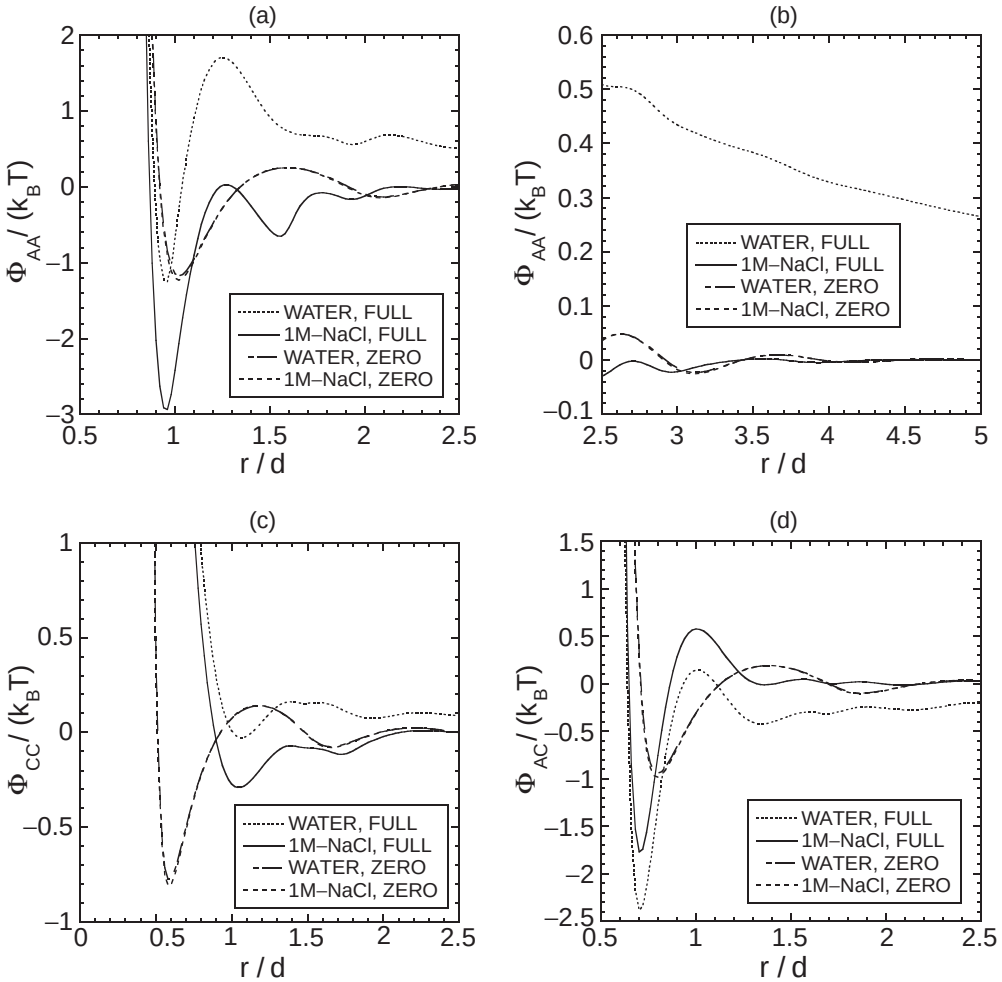


Fig. 3. Potential of mean force scaled by $k_BT$ ($d = 0.28$ nm). "Full" means that the full values of the partial charges are assigned to the solute atoms. "Zero" means that the partial charges are set at zero. (a) For the A–A pair at small separations. (b) For the A–A pair at large separations. (c) For the C–C pair. (d) For the A–C pair.

$\Phi_{CC}(r)/(k_BT)$ is plotted in Fig. 3c. Two cases, where the full partial charge is assigned to atom C and where the charge is set at zero, respectively, are considered. In the case of full charges in pure water, $\Phi_{CC}(r)/(k_BT)$ is repulsive at almost all separations and it converges rather slowly to $u_{CC}(r)/(\varepsilon_W k_BT)$. The salt effects are qualitatively similar to those observed for $\Phi_{AA}(r)/(k_BT)$, though the contact atom pair is unstable and the first minimum corresponds to the solvent-separated atom pair.[3,4] When $q_C$ is set at zero and the electrostatic repulsion is removed, the atoms come much closer to each other due to their small sizes. Large stabilization occurs at contact, which is absent in the case of full charges in salt solution.

$\Phi_{AC}(r)/(k_BT)$ is plotted in Fig. 3d. Two cases, where the full partial charges are assigned to the atoms and where the charges are set at zero, respectively, are considered. In the case of full charges in pure water, $\Phi_{AC}(r)/(k_BT)$ is attractive except at some small separations and it converges rather slowly to $u_{AC}(r)/(\varepsilon_W k_BT)$. By the salt addition, $\Phi_{AC}(r)/(k_BT)$ exhibits an upward shift due to the enhanced solvation. It becomes short range and rapidly converges to zero. The DRISM theory overestimates the depth of the first minimum of $\Phi_{AC}(r)/(k_BT)$ both in pure water and in salt solution,[3,4] but the difference between the two curves is quantitatively reliable. The first and second minimums correspond to the contact atom pair and the solvent-separated atom pair, respectively.[3,4] Again, the PMF for the zero charges in pure water is considerably different from that for the full charges in salt solution.

The pair correlation functions for solute atoms with partial charges, $g_{A+}(r)$ and $g_{C-}(r)$, have sharp first peaks, indicating the preferential binding of counterions. Figures 4a and 4b show $\delta g_{C-}(r;R)$ (see Eq. 10) for the C–C pair and $\delta g_{C-}(r;R)$ for the A–C pair, respectively. For the C–C pair $\delta g_{C-}(r;R)$ becomes progressively larger as the two solute atoms approach each other. For the A–C pair, $\delta g_{C-}(r;R)$ at small $r$ exhibits an oscillation against the change in $R$, but as a whole it takes a larger, negative value as the two solute atoms approach each other. The binding of anions to a positively charged solute atom becomes stronger with decreasing $R$ when the partial charge of the partner solute atom is positive, while it becomes weaker when the partner carries a negative partial charge.

If the charges of solute atoms are set at zero and the atoms are considered in pure water, the PMF exhibits a pattern of the hydrophobic interaction. It is much closer to the PMF for the

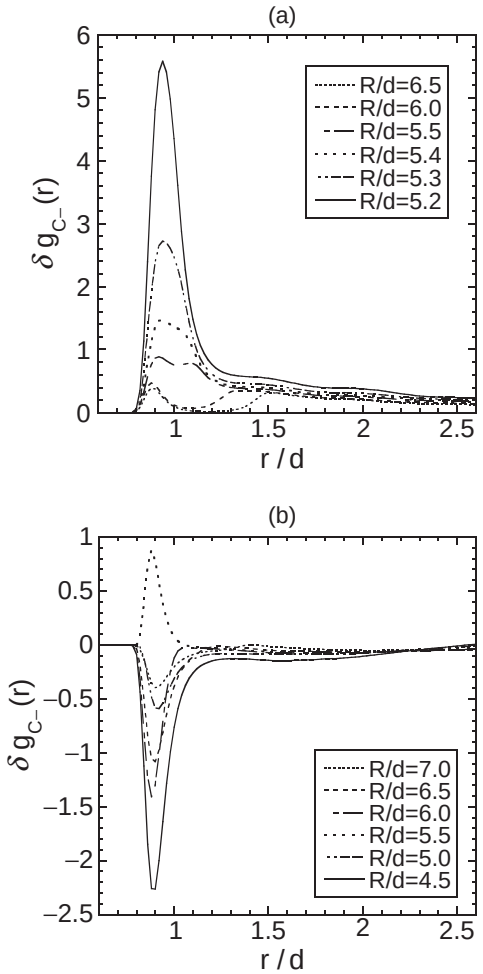


Fig. 4. The function $\delta g_{C-}(r;R)$ defined by Eq. 10 in 1 M-NaCl solution ($d = 0.28$ nm). The anions are chloride ions. (a) For the C–C pair. (b) For the A–C pair.

full charges in salt solution than to that for the full charges in pure water in the sense that it is short range. However, at small separations it is quite different from the PMF for the full charges in salt solution. It is true that in salt solution the atomic charges are screened by the counterions, but considering the screening effects by setting the charges at zero and immersing the atoms in pure water gives no good approximation.

**Effects Due to Salt Concentration.** The behavior of the PMF is strongly dependent on the salt concentration, as illustrated for $\Phi_{AA}(r)/(k_BT)$ in Figs. 5a and 5b. The salt is NaCl and the full charge is assigned to atom A. The addition of increasing concentration of salt gradually leads from repulsive to attractive interactions. Even at the lowest concentration 0.1 M, the PMF exhibits a significantly large, downward shift and becomes much shorter range. When the salt concentration is sufficiently high (>1 M), the PMF is attractive at all separations except in the region where the direct core repulsion dominates. As Figure 5c shows, $\Phi_{CC}(r)/(k_BT)$ exhibits a similar change for the increase in the salt concentration. This suggests that the qualitative aspects of the conclusions are dependent neither on the solute sizes nor on the magnitudes of partial charges.

$\Phi_{AC}(r)/(k_BT)$ as a function of the salt concentration is illustrated in Fig. 5d. The salt is NaCl and the full charges are assigned to atom A and to atom C. The addition of increasing concentration of salt gradually leads from attractive to repulsive interactions. When the salt concentration is sufficiently high (>1 M), the PMF is repulsive except in the narrow region near the first minimum. Since the DRISM theory overestimates the depth of the first minimum of $\Phi_{AC}(r)/(k_BT)$,[1,2] the accurate PMF in the narrow region should be more repulsive.

**Physical Interpretation of the Observed Salt Effects.** The very small separations where the core repulsion dominates are excluded from the discussion. The PMF is "the system free energy in the state where centers of the solute atoms are separated by distance $r$"−"the system free energy in the state where the solute atoms are infinitely separated". It is convenient to decompose the solvation $s(r)$ into its energetic and entropic components:

$$s(r) = s_E(r) + \{-Ts_S(r)\}. \tag{13}$$

The PMF can then be written as

$$\Phi(r)/(k_BT) = u(r)/(k_BT) + s_E(r) + \{-Ts_S(r)\}. \tag{14}$$

Kovalenko and Hirata[3,4] calculated $\{u(r)/(k_BT) + s_E(r)\}$ and $\{-Ts_S(r)\}$ for like- and unlike-charged ions in pure water and showed that the magnitude of the former is comparable with that of the latter. This means that $s_E(r)$ for like-charged ions is largely negative (strongly attractive) while $s_E(r)$ for unlike-charged ions is largely positive (strongly repulsive). Note that $|u(r)/(k_BT)|$ and $|s_E(r)|$ are much larger than $|\{-Ts_S(r)\}|$. They also showed that $\{-Ts_S(r)\}$ is positive for like-charged ions while it is negative for unlike-charged ions. In the next two paragraphs, we give physical interpretations of the results calculated by Kovalenko and Hirata,[3,4] which were not described in their articles, and of the salt effects observed in our analysis.

The observation that the direct interaction and the solvation are opposing is ascribed to the feature that $u(r)/(k_BT)$ and $s_E(r)$ are opposing. As the solute atoms with like partial charges approach each other, the direct interaction $u(r)/(k_BT)$ becomes more repulsive. However, the electric field near the solute atoms increases as they approach each other. First, let us consider the solvation in pure water. As a result of the increased electric field, hydrogen atoms (with positive partial charges) or oxygen atoms (with negative partial charges) of water molecules are more strongly attracted to the solute atoms and the stabilization by the electrostatic interaction becomes larger, leading to more negative $s_E(r)$. The more ordered arrangement of water molecules gives rise to more positive $\{-Ts_S(r)\}$. An important point is that $s_E(r)$ is not strong enough to cancel $[u(r)/(k_BT) + \{-Ts_S(r)\}]$. The reason for this is that when oxygen atoms come closer to solute atoms with positive partial charges, for example, hydrogen atoms also come closer unavoidably. We now discuss the solvation in salt solution. When salt is added to water, anions are attracted to the solute atoms with positive partial charges with very few cations accompanying the anions. Thus, the electrostatic stabilization arising from the increased electric field becomes larger (i.e., the sensitivity to a change in the strength of the electric field is higher) than in pure water. This leads to even more negative $s_E(r)$ and more positive $\{-Ts_S(r)\}$. The result, the PMF exhibits a downward shift by the salt addition, indicates that the change in $s_E(r)$

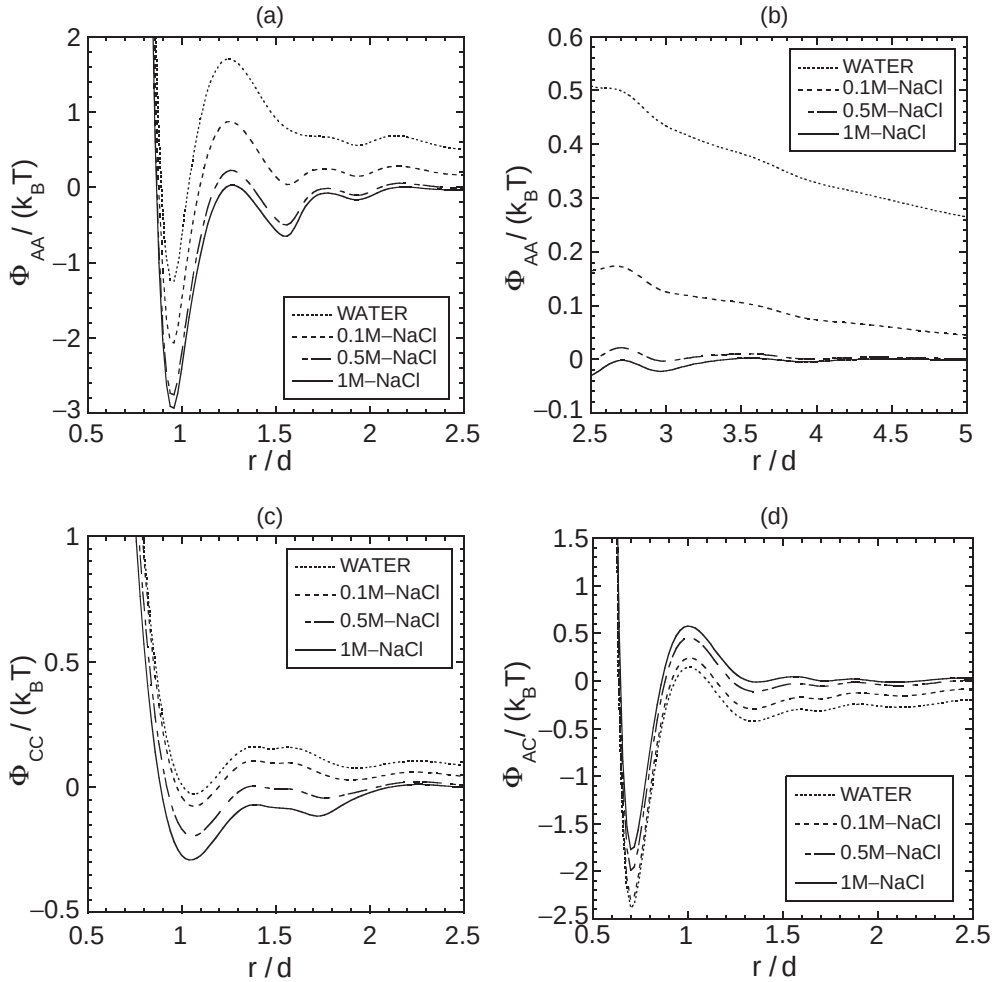


Fig. 5. Salt-concentration effects on potential of mean force scaled by $k_BT$ ($d = 0.28$ nm). The salt is NaCl and the full values of the partial charges are assigned to the solute atoms. (a) For the A–A pair at small separations. (b) For the A–A pair at large separations. (c) For the C–C pair. (d) For the A–C pair.

dominates and $s(r)$ becomes more negative (i.e., the solvation becomes stronger). As the salt concentration increases, the solvation becomes progressively stronger and eventually surpasses the direct interaction. When the salt concentration is sufficiently high, at all separations the solvation predominates over the direct interaction and the PMF becomes attractive. As the partial charge increases, both the direct interaction and the solvation become stronger. In pure water, the enhancement of the former dominates and the PMF becomes more repulsive. In salt solution, by contrast, if the salt concentration is sufficiently high, the enhancement of the solvation dominates, leading to a shift of the PMF in a more attractive direction. A result showing this is presented in the next section.

When solute atoms with unlike partial charges approach each other, $u(r)/(k_BT)$ becomes more attractive. However, the electric field near each of the solute atoms decreases as they approach each other. As a result, in pure water, hydrogen or oxygen atoms of water molecules are less strongly attracted to the solute atoms and the stabilization by the electrostatic interaction becomes smaller, leading to more positive $s_E(r)$. The less ordered arrangement of water molecules leads to more negative $\{-Ts_S(r)\}$. In pure water $[u(r)/(k_BT) + \{-Ts_S(r)\}]$ is generally dominant. When salt is added to water, due to the higher sensitivity to a change in the strength of the electric field, $s_E(r)$ becomes even more negative and $\{-Ts_S(r)\}$ becomes more negative. The result, that the PMF exhibits an upward shift by the salt addition, indicates that the change in $s_E(r)$ dominates and $s(r)$ becomes more positive. As the salt concentration increases, the solvation becomes progressively stronger. When the salt concentration is sufficiently high, except in the narrow region near the first minimum, the solvation is dominant and the PMF becomes repulsive.

**Effects Due to Salt Species.** The size of the counterions has large effects on the PMF. $\Phi_{AA}(r)/(k_BT)$ in 1 M-KCl solution is compared with $\Phi_{AA}(r)/(k_BT)$ in 1 M-NaCl solution in Fig. 6a. The PMF in pure water is also included in the Figure. The full charge is assigned to atom A. The downward shift caused by the salt addition is more pronounced for NaCl than for KCl. The coordination number (see Eq. 11) of cations around atom A calculated is $n_+ = 0.558$ for $Na^+$ and $n_+ = 0.164$ for $K^+$. Thus, the ability of cations to change the PMF between solute atoms with negative partial charges follows the order $Na^+ > K^+$: The ability is higher for a smaller ionic size. The coordination number, which gives a measure of the

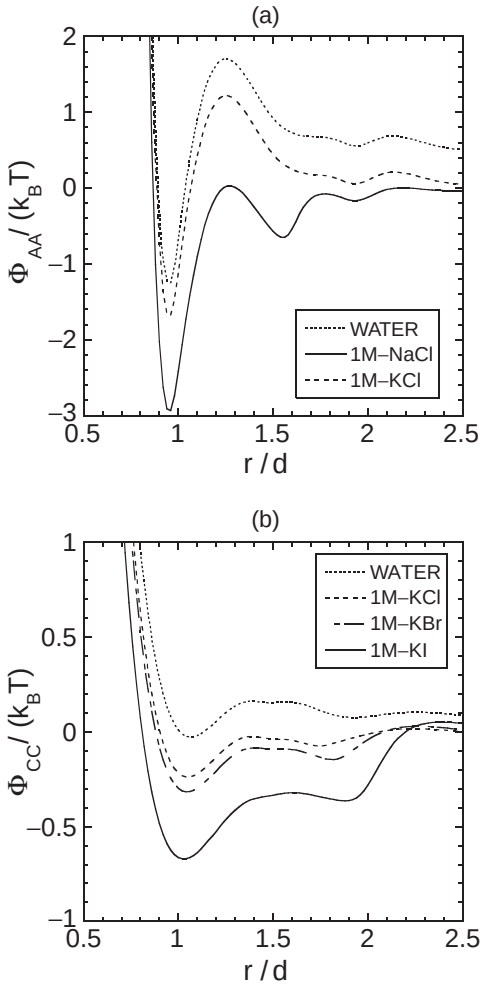


Fig. 6. Effects due to size of counterions on potential of mean force scaled by $k_BT$ ($d = 0.28$ nm). The full values of the partial charges are assigned to the solute atoms. (a) For the A–A pair. (b) For the C–C pair.

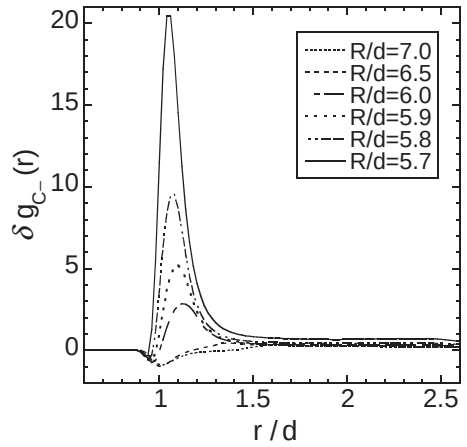


Fig. 7. The function $\delta g_{C-}(r;R)$ defined by Eq. 10 for the C–C pair in 1 M-KI solution ($d = 0.28$ nm). The anions are iodide ions.

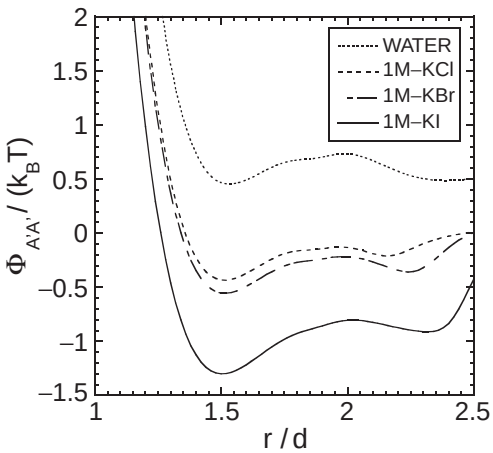


Fig. 8. Effects due to size of counterions (anions) on potential of mean force scaled by $k_BT$, $\Phi_{A'A'}(r)/(k_BT)$, for the A′–A′ pair ($d = 0.28$ nm). The partial charge of atom A′ is positive ($= 0.721$).

strength of cation binding, follows the same order.

The effects of anion species on $\Phi_{CC}(r)/(k_BT)$ are illustrated in Fig. 6b. The PMF in pure water is also included in the Figure. The full charge is assigned to atom C. The downward shift of the PMF becomes more pronounced as the anion size increases. The coordination number of anions around atom C calculated is $n_- = 0.309$ for $Cl^-$, $n_- = 0.430$ for $Br^-$, and $n_- = 0.543$ for $I^-$. Figure 7 shows $\delta g_{C-}(r;R)$ for the C–C pair in 1 M-KI solution. As the two solute atoms approach each other, the binding of iodide ions becomes increasingly stronger. This is more remarkable than in the case of the binding of chloride ions shown in Fig. 4b. To assure the effects due to anion species observed, new calculations have been performed. The partial charge of atom A is multiplied by $-1$ (i.e., the charge is now positive) with the other parameters unchanged and this solute atom is referred to as atom A′. The effects of anion species on $\Phi_{A'A'}(r)/(k_BT)$ are illustrated in Fig. 8. The downward shift of the PMF certainly becomes more pronounced as the anion size increases. Thus, the ability of anions to change the PMF between solute atoms with positive partial charges follows the order $I^- > Br^- > Cl^-$, which is opposite to the Hofmeister series: The ability becomes higher as the ionic size increases. The coordination number, which gives a measure of the strength of anion binding, follows the same order. The effects due to the magnitude of the partial charge can be understood by comparing Fig. 6b and Fig. 8. As the magnitude increases, the PMF in pure water becomes more repulsive, whereas the PMF in salt solution becomes more attractive. The downward shift is particularly appreciable in the case of KI.

As expected, the effects of anion species on $\Phi_{AA}(r)/(k_BT)$ (these are illustrated in Fig. 9) and those of cation species on $\Phi_{CC}(r)/(k_BT)$ are small. The ability of ions to shift the PMF in a more attractive direction and to make it much shorter range follows the orders: $Na^+ > K^+$ and $Cl^- > Br^- > I^-$. The ability becomes higher as the ionic size decreases for both the cations and the anions.

The partial charge of atom C is set at zero and $\Phi_{CC}(r)/(k_BT)$ is calculated for 1 M-NaCl, KCl, KBr, and KI solutions. The PMF between solute atoms with zero partial charges in salt solution is only slightly different from the PMF in pure water.

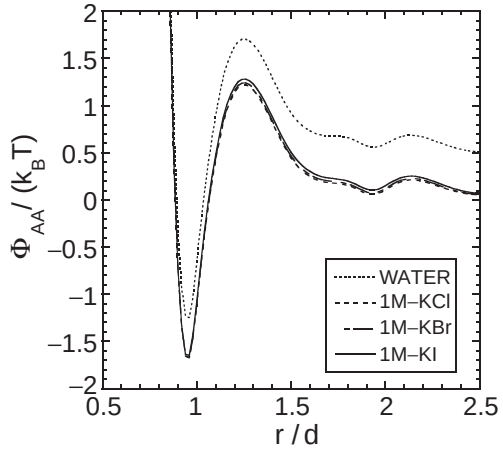


Fig. 9. Effects due to size of anions on potential of mean force scaled by $k_BT$, $\Phi_{AA}(r)/(k_BT)$, for the A–A pair ($d = 0.28$ nm). The full value of the partial charge is assigned to atom A.

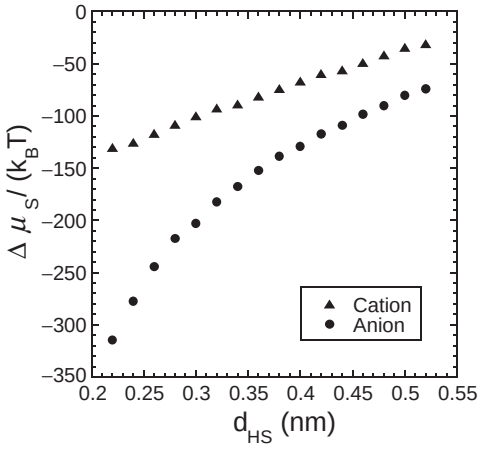


Fig. 10. Hydration free energy scaled by $k_BT$ of a hard-sphere ion carrying a positive or negative charge in pure water. In calculating the water-ion potentials, the oxygen atom and the hydrogen atom are regarded as hard spheres of 0.28 nm and 0.04 nm in size, respectively (the partial charges are given in Table 2). The curve formed by the triangles or the circles is not smooth. This is because the grid width $\delta r$ in the numerical treatment is finite and the water-ion hard-sphere repulsions are not accurately treated.

Overall, the salt addition leads to a minor, downward shift of the PMF, which is indicative of enhanced hydrophobicity. The ability of salt to shift the PMF follows the order: NaCl > KCl > KBr > KI. The ability becomes higher as the ionic size decreases for both the cations and the anions. This result can be interpreted as follows. The structure of solution becomes more rigid due to the salt addition[21] and the work required to create a cavity large enough to accommodate a hydrophobic solute molecule increases, leading to the enhanced hydrophobicity. Smaller ions are more strongly hydrated, giving rise to the greater rigidity of the solution structure. It follows that the ability of ions in decreasing the solubility of noble gases[13,17] and hydrophobic molecules such as benzene[22,23] follows the order: $Na^+ > K^+$ and $Cl^- > Br^- > I^-$, which is consistent with the Hofmeister series.

**Physical Interpretation of the Observed Effects Due to Cationic and Anionic Sizes.** As mentioned above, the change in the PMF caused by the salt addition is governed by the change in $s_E(r)$. The counterions bind to solute atoms with large partial charges and the solvation is enhanced. The stronger the binding is, the larger the PMF change is. However, the degree of the binding depends on the size of the counterions. The degree could be determined by the competition of two major factors. These are the work required to destroy the hydration shells of counterions (factor 1) and the energy gain (i.e., stabilization by the direct electrostatic attractive interaction) that occurs when the counterions bind to the solute atoms (factor 2). From the standpoint of factor 1, smaller counterions are more strongly hydrated, leading to more work required and weaker binding. From the standpoint of factor 2, smaller counterions can get closer to the solute atoms, resulting in more energy gain and stronger binding.

The results from a theoretical analysis on the salt-species effects can be dependent on the size parameters chosen for the ions and the solute atoms. Under the calculation conditions described above, the cations ($Na^+$ and $K^+$) and the anions ($Cl^-$, $Br^-$, and $I^-$) behave differently. When the ionic size becomes larger, both factor 1 and factor 2 decrease, but for the cations the decrease in factor 2 is dominant, with the result of the weaker binding. For the anions, the decrease in factor 1 dominates and the binding of a larger anion is stronger. The ability of counterions to change the PMF follows the orders: $Na^+ > K^+$ and $I^- > Br^- > Cl^-$. With the conventional model treating water as the dielectric continuum, the electrostatic interaction between a counterion and a solute atom is simply the direct Coulomb potential divided by $\varepsilon_W$. This implies that smaller counterions always bind to the solute atoms more strongly, leading to the opposite result for the anions. The ion-size effects can correctly be described only by employing the molecular model for water.

The hydration free energy $\Delta\mu_S$ of a hard-sphere ion carrying a positive or negative charge in pure water is calculated as a function of the hard-sphere diameter $d_{HS}$. The result is plotted in Fig. 10. The absolute value of $\Delta\mu_S$ represents the strength of the hydration and could be a measure of the work required to destroy the hydration shell of an ion (this is described above as factor 1), and the value of $\sigma$ roughly corresponds to $d_{HS}$. As $d_{HS}$ becomes larger, both $|\Delta\mu_S|$ and the slope decrease. Anions are usually larger than cations, but for a given value of $d_{HS}$, $|\Delta\mu_S|$ and the slope for anions are much larger than for cations. The difference between $Na^+$ and $K^+$ in the value of $\sigma$ is 0.088 nm, and the increase of $d_{HS}$ from 0.226 nm (the value of $\sigma$ of $Na^+$) by this amount leads to $|\Delta\mu_S|$ that is ~20 kcal/mol smaller. The value of $\sigma$ of $I^-$ is 0.062 nm larger than that of $Cl^-$, and the increase of $d_{HS}$ from 0.392 nm (the value of $\sigma$ of $Cl^-$) by this amount leads to $|\Delta\mu_S|$ that is ~21 kcal/mol smaller. The numbers, 20 and 21, are almost the same. The energy gain, which occurs when an ion binds to a solute atom (the size of atom A and atom A′ is 0.285 nm) with a partial charge in the opposite sign (this is described above as factor 2), decreases both when $d_{HS}$ increases from 0.226 nm by 0.088 nm and when $d_{HS}$ increases from 0.392 nm by 0.062 nm. However, the decrease in the for-

mer is more pronounced. Though the effects due to the ionic sizes are to be investigated more extensively in future studies, we suggest that, when the ionic size increases, for the anions the decrease in factor 1 is dominant and the binding becomes stronger whereas for the cations the decrease in factor 2 is dominant and the binding becomes weaker.

## Relevance to Conformational Transition of Biomolecules

**Conformational Transition and Solubility Change for Peptides and Proteins with Many Positively Charged Groups in Side Chains.** We limit our discussions to the effects due to monovalent anions. It was experimentally observed that $\beta$-lactamase, cytochrome *c*, and apomyoglobin are extremely unfolded under conditions of pH $\sim$ 2 and low ionic strength, but they are refolded to molten-globule-like conformations by the salt addition.[8,9] Although melittin at micromolar concentrations is unfolded under conditions of low ionic strength and neutral pH, it adopts a tetrameric helical structure when salt is added to the solution. The ability of salt to cause the conformational transition is strongly dependent on anion species and follows the order $I^- > Br^- > Cl^-$. It was found by another group[24–26] that the solubility of lysozyme is greatly decreased by the salt addition. A finding is that the efficiency of anions in decreasing the solubility of lysozyme at pH $\sim$ 4.5 is strong and follows the order $I^- > Br^- > Cl^-$, whereas that of cations is weak. They also used small-angle X-ray scattering for lysozyme to characterize the salt effects on the protein–protein interactions and observed that the addition of increasing concentration of salt gradually leads from repulsive to attractive interactions.[24] Recently, Henkels et al.[27] investigated an anion-induced folding of the P protein and reported that the effectiveness of anions in stabilizing the folded protein follows the order $I^- > Br^- > Cl^-$, while cations have almost no effects.

The results of our theoretical analysis show that the PMF between solute atoms with large, like partial charges exhibits a drastic change when salt is added to water. It becomes attractive at all separations under the condition of sufficiently high salt concentration. When the partial charges are positive, the ability of salt to cause the PMF change is strongly dependent on anion species and follows the order $I^- > Br^- > Cl^-$. Since these properties originate exclusively from electrostatics, they are generally applicable to the interaction between positively charged groups and are relevant to the experimental results mentioned above. The repulsive interactions among positively charged groups in the side chains immersed in pure water often induce a protein molecule to take a less compact, unfolded conformation. Our results indicate that the interactions change into attractive ones due to the salt addition and that the conformational transition to a more compact, folded conformation is caused. The overall protein–protein interactions also become far more attractive and drive the protein molecules to aggregate, leading to a decrease in the protein solubility. The ability of salt to cause the conformational transition and the solubility decrease is strongly dependent on anion species and follows the order $I^- > Br^- > Cl^-$. The qualitative aspects of the experimental observations[8–10,24–27] can thus be explained.

**B–Z Transition of DNA.** An interesting example of an induced DNA structural transition in aqueous solution is the right-to-left (B–Z) transition of d[(G–C)] polymers and oligomers induced by increasing salt concentration.[11,12] The ability of salt to cause the structural transition is strongly dependent on cation species[12] and follows the order: $Na^+ > K^+ > Rb^+ > Cs^+$. For example, the transition from the B-form to the Z-form occurs at $\sim$2.3 M for NaCl and at $\sim$4.7 M for CsCl. Hirata and Levy[28] considered the B–Z transition of DNA, but their work had two aspects to be improved: They treated water as a dielectric continuum and the effects due to the cationic size were not discussed. Soumpasis[29] dealt with the cationic size effects but he employed the dielectric continuum model for water.

The results of our theoretical analysis suggest that the PMF between negatively charged groups becomes progressively more attractive as the salt concentration increases. With increasing salt concentration, contacts of negatively charged groups are more stabilized or negatively charged groups are driven to become closer together. In our view, the major geometric difference between B-DNA and Z-DNA with regard to electrostatic properties is that the negatively charged phosphates are relatively much closer together in Z-DNA.[30] It is expected that, when the concentration is sufficiently high, the solvation free energy of the Z-form will become considerably lower than that of the B-form from the electrostatic viewpoint. Considering our results, we can infer that the ability of cations to cause the structural transition becomes higher as the cationic size decreases, which is opposite to the case of 3.1 in terms of the ion-size effects. These results are qualitatively in good accord with the experimental observations[11,12] mentioned above.

## Concluding Remarks

We have analyzed the potential of mean force (PMF) between solute atoms with like, unlike, or zero partial charges immersed in pure water and in solutions of various salts (NaCl, KCl, KBr, and KI) using the dielectrically consistent reference interaction site model (DRISM) theory. As for the PMF between solute atoms with like partial charges, the addition of increasing concentration of salt gradually leads from repulsive to attractive interactions. The most striking result is that when the salt concentration becomes sufficiently high, the contact of like-charged atoms is stabilized. Moreover, the stability is even enhanced as the magnitude of the partial charge increases. For positive charges, the ability of salt to change the PMF is governed by anion species and follows the order $I^- > Br^- > Cl^-$: The ability becomes higher as the anionic size increases. For negative charges, by contrast, the ability becomes higher as the cationic size decreases and follows the order $Na^+ > K^+$. As for the PMF between solute atoms with unlike charges, the addition of increasing concentration of salt gradually leads from attractive to repulsive interactions. The contact of unlike-charged atoms is less stabilized than in pure water. It is interesting to note that, in salt solution, the PMF between like-charged solute atoms can be considerably more attractive than the PMF between unlike-charged solute atoms.

Some qualitative aspects of the salt-induced conformational transition and the solubility change experimentally observed for biomolecules are completely independent of specific chemical or conformational properties of individual biomolecules.

As the first step of the research, it is reasonable to deal with such general aspects rather than with specific details. In the present article, we have given physical insights into the results of our analysis, which are fairly general. We have then discussed the relevance to the salt effects for two typical examples in which like-charged groups are driven to become closer together by the salt addition. The first example is the conformational transition and the solubility decrease caused by the salt addition for peptides and proteins with many positively charged groups in the side chains, and the second one is the salt-induced B–Z transition of DNA with many negatively charged phosphates. In the first example, the ability of salt to cause the conformational transition is strongly dependent on anion species and follows the order $I^- > Br^- > Cl^-$. In the second example, the ability of salt to cause the structural transition is strongly dependent on cation species and follows the order $Na^+ > K^+ > Rb^+ > Cs^+$. The ability becomes higher as the anionic size increases in the first example, whereas in the second one it becomes higher as the cationic size decreases. These experimental observations are qualitatively in good agreement with our theoretical results.

We thank F. Hirata, Y. Goto, and T. Imai for fruitful discussions and A. Kovalenko for sending us the numerical data plotted in Fig. 1. This work was supported by a Grant-in-Aid for Scientific Research on Priority Areas (No. 15076203) from the Ministry of Education, Culture, Sports, Science and Technology of Japan and by NAREGI Nanoscience Project.

## References

1 B. M. Pettitt and M. Karplus, *Chem. Phys. Lett.*, **121**, 194 (1985).
2 P. E. Smith, B. M. Pettitt, and M. Karplus, *J. Phys. Chem.*, **97**, 6907 (1993).
3 A. Kovalenko and F. Hirata, *J. Chem. Phys.*, **112**, 10391 (2000).
4 A. Kovalenko and F. Hirata, *J. Chem. Phys.*, **112**, 10403 (2000).
5 J. S. Perkyns and B. M. Pettitt, *J. Chem. Phys.*, **97**, 7656 (1992).
6 M. Kinoshita, Y. Okamoto, and F. Hirata, *J. Comput. Chem.*, **18**, 1320 (1997).
7 M. Kinoshita, Y. Okamoto, and F. Hirata, *J. Comput. Chem.*, **19**, 1724 (1998).
8 Y. Goto, N. Takahashi, and A. L. Fink, *Biochemistry*, **29**, 3480 (1990).
9 Y. Hagihara, M. Kataoka, S. Aimoto, and Y. Goto, *Biochemistry*, **31**, 11908 (1992).
10 Y. Goto and S. J. Nishikiori, *J. Mol. Biol.*, **222**, 679 (1991).
11 F. M. Pohl and T. M. Jovin, *J. Mol. Biol.*, **67**, 375 (1972).
12 D. M. Soumpasis, M. Robert-Nicoud, and T. M. Jovin, *FEBS Lett.*, **213**, 341 (1987).
13 T. Imai, M. Kinoshita, and F. Hirata, *Bull. Chem. Soc. Jpn.*, **73**, 1113 (2000).
14 H. J. C. Berendsen, J. R. Grigera, and T. P. Straatsma, *J. Phys. Chem.*, **91**, 6269 (1987).
15 B. M. Pettitt and P. J. Rossky, *J. Chem. Phys.*, **77**, 1451 (1982).
16 B. M. Pettitt and P. J. Rossky, *J. Chem. Phys.*, **84**, 5836 (1986).
17 M. Kinoshita and F. Hirata, *J. Chem. Phys.*, **106**, 5202 (1997).
18 H. A. Yu and M. Karplus, *J. Chem. Phys.*, **89**, 2366 (1988).
19 W. L. Masterton and T. P. Lee, *J. Phys. Chem.*, **74**, 1776 (1970).
20 S. J. Singer and D. Chandler, *Mol. Phys.*, **55**, 621 (1985).
21 R. Leberman and A. K. Soper, *Nature*, **378**, 364 (1995).
22 W. F. McDevit and F. A. Long, *J. Am. Chem. Soc.*, **74**, 1773 (1952).
23 R. L. Baldwin, *Biophys. J.*, **71**, 2056 (1996).
24 M. Riès-Kautt and A. Ducruix, *Methods Enzymol.*, **276**, 23 (1997).
25 M. Riès-Kautt and A. Ducruix, *J. Biol. Chem.*, **264**, 745 (1989).
26 J.-P. Guilloteau, M. Riès-Kautt, and A. Ducruix, *J. Cryst. Growth*, **122**, 223 (1992).
27 C. H. Henkels, J. C. Kurz, C. A. Fierke, and T. G. Oas, *Biochemistry*, **40**, 2777 (2001).
28 F. Hirata and R. M. Levy, *J. Phys. Chem.*, **93**, 479 (1989).
29 D. M. Soumpasis, *Proc. Natl. Acad. Sci. U.S.A.*, **81**, 5116 (1984).
30 A. H.-J. Wang, G. J. Quigley, F. J. Kolpak, J. L. Crawford, J. H. van Boom, G. van der Marel, and A. Rich, *Nature*, **282**, 680 (1979).